



**HAL**  
open science

# Time window for magnetic reconnection in plasma configurations with velocity shear

Matteo Faganello, F. Califano, F. Pegoraro

► **To cite this version:**

Matteo Faganello, F. Califano, F. Pegoraro. Time window for magnetic reconnection in plasma configurations with velocity shear. *Physical Review Letters*, 2008. hal-02315150

**HAL Id: hal-02315150**

**<https://hal.science/hal-02315150v1>**

Submitted on 14 Oct 2019

**HAL** is a multi-disciplinary open access archive for the deposit and dissemination of scientific research documents, whether they are published or not. The documents may come from teaching and research institutions in France or abroad, or from public or private research centers.

L'archive ouverte pluridisciplinaire **HAL**, est destinée au dépôt et à la diffusion de documents scientifiques de niveau recherche, publiés ou non, émanant des établissements d'enseignement et de recherche français ou étrangers, des laboratoires publics ou privés.

M. Faganello, F. Califano, F. Pegoraro  
*Physics Dept., University of Pisa, Pisa, Italy*

It is shown that the rate of magnetic field line reconnection can be clocked by the evolution of the large scale processes that are responsible for the formation of the current layers where reconnection can take place. In unsteady plasma configurations, such as those produced by the onset of the Kelvin-Helmholtz instability in a plasma with a velocity shear, qualitatively different magnetic structures are produced depending on how fast the reconnection process develops on the external clock set by the evolving large scale configuration.

PACS numbers: 52.35.Vd, 52.35.Mw, 52.65.Kj, 52.35.Py

Fast magnetic field line reconnection is believed to be a crucial phenomenon in low collisionality or collisionless plasmas, as expected to occur on time scales that do not exceed by large factors the dynamical plasma time scales as determined within the ideal magnetohydrodynamic (MHD) description. When current layers are formed that have widths of order of the ion skin depth  $d_i \equiv c/\omega_{pi}$ , with  $\omega_{pi}$  the ion plasma frequency, ions inside these current layers decouple their motion from the evolution of the magnetic field. *Per se* this decoupling is not sufficient to allow for magnetic reconnection which requires electron decoupling. This latter occurs inside a thinner region that, depending on the plasma parameters, has a width determined either by a non-vanishing resistivity or by kinetic effects, or, as is the two fluids model description adopted here, by electron inertia effects. The large spatial separation between these two decoupling regions allows magnetic reconnection to grow at a faster rate [1–5].

In a magnetized plasma streaming with a nonuniform velocity, the Kelvin-Helmholtz (K-H) instability plays a major role in mixing different plasma regions and in stretching the magnetic field lines leading to the formation of layers with a sheared magnetic field where magnetic field line reconnection can take place. A relevant example is provided by the formation of a mixing layer between the Earth’s magnetosphere and the solar wind at low latitudes during northward periods recently investigated in Ref. [6] (see also references therein). In the considered configuration, in the presence of a magnetic field nearly perpendicular to the plane defined by the velocity field and its inhomogeneity direction, velocity shear drives a K-H instability which advects and distorts the magnetic field configuration. If the Alfvén velocity associated to the in-plane magnetic field is sufficiently weak with respect to the variation of the fluid velocity in the plasma, the K-H instability generates fully rolled-up vortices which advect the magnetic field lines into a complex configuration, causing the formation of current layers. Since the plasma dynamics is essentially driven by the vortex motion, the reconnection events that are produced in these layers are usually denoted as Vortex

Induced Reconnection (VIR) [7–11].

Pairing of the vortices generated by the K-H instability is a well know phenomenon in two-dimensional hydrodynamics [12, 13]. On the other hand, the role of the magnetic field on vortex dynamics has been studied essentially in the limit of only one vortex, the largest one contained in the simulation box. It has been shown that, even if the magnetic field is weak and unable to prevent the formation of the KH vortex, nevertheless the VIR process eventually leads to vortex disruption [9, 10, 14]. On the contrary, in this letter we investigate the development of magnetic reconnection during the vortex pairing process and show that completely different large scale magnetic structures are produced depending on how fast the reconnection process develops on the time scale set by the pairing process. We consider a configuration with a value of the plasma  $\beta$  parameter (ratio of plasma pressure over total magnetic field pressure) of order unity and show that in this regime the Hall term in Ohm’s law, corresponding to the decoupling of electrons and ions inside the current layers, allows magnetic reconnection to occur on time scales fast enough to compete with the pairing process. In our simulations, the conditions for magnetic reconnection are provided, in an initially uniform in-plane magnetic field, by the motion of the K-H vortices that grow and pair in the initially imposed shear velocity field. We observe that VIR does not destroy the vortices before they coalesce, in agreement with multiple vortices study in a homogeneous plasma [8]. We find that if the Hall term is removed from Ohm’s law, the development of reconnection, and thus eventually of the K-H vortices, is qualitatively, not only quantitatively, different. This result provides a clear cut example of the feedback between large and small scale physics, as the necessary conditions for reconnection to occur are produced by the large scale vortex motion, but the specific physical processes that make reconnection act faster or slower determine eventually the evolution of the entire system and the final magnetic field structure.

We consider a 2D description of the system, with the inhomogeneity direction along  $x$ , the periodic direction along  $y$ , and  $z$  an ignorable coordinate. We adopt a

two-fluid, quasineutral plasma model. The corresponding dimensionless set of equations, normalized to the ion cyclotron frequency  $\Omega_{ci}$  and to the ion skin depth  $d_i$  ( $d_e^2 = m_e/m_i$ ), reads:  $\partial n/\partial t + \nabla \cdot (n\mathbf{U}) = 0$  where  $n$  is the plasma density,  $\mathbf{U} = (\mathbf{u}_i + d_e^2 \mathbf{u}_e)$  the fluid velocity and  $u_{i,e}$  the ion and electron fluid velocities,

$$\partial(n\mathbf{U})/\partial t + \nabla \cdot [n(\mathbf{u}_i \mathbf{u}_i + d_e^2 \mathbf{u}_e \mathbf{u}_e) + (P\bar{\mathbf{I}} - \mathbf{B}\mathbf{B})] = 0, \quad (1)$$

with  $P = P_i + P_e + B^2/2$  taken spatially uniform at  $t = 0$  and isothermal closures  $P_{i,e} = nT_{i,e}$ . The magnetic field  $\mathbf{B}$  is advanced by solving the Faraday equation and the electric field  $\mathbf{E}$  is calculated by means of the following generalized Ohm's law [15],

$$\begin{aligned} (1 - d_e^2 \nabla^2) \mathbf{E} &= -\mathbf{u}_e \times \mathbf{B} \\ -d_e^2 \{ \mathbf{u}_i \times \mathbf{B} + (1/n) \nabla \cdot [n(\mathbf{u}_i \mathbf{u}_i - \mathbf{u}_e \mathbf{u}_e)] \} \end{aligned} \quad (2)$$

where the term  $\nabla P_e/n$  has been omitted since, for a polytropic equation of state, it does not contribute to  $\nabla \times \mathbf{E}$ . **Electron and ion velocities are obtained by combining the fluid velocity  $\mathbf{U}$ , Eq. (1), and the current  $\mathbf{J} \equiv n(\mathbf{u}_i - \mathbf{u}_e) = \nabla \times \mathbf{B}$  (where we neglect the displacement current).**

We consider an initial large-scale, sheared velocity field:  $\mathbf{U}_{eq} = (U_0/2) \tanh[(x - L_x/2)/L_u] \hat{\mathbf{y}}$ . Since we are interested in the VIR process, we consider a homogeneous density in order to eliminate other secondary fluid instabilities [16, 17]. The equilibrium magnetic field at  $t = 0$  is homogeneous:  $\mathbf{B}_{eq}(x, y) = B_{y,eq} \mathbf{e}_y + B_{z,eq} \mathbf{e}_z$ . We take  $L_u = 3.0$  and a box-length  $L_x = 90$  in the  $x$  direction and  $L_y = 30\pi$  in the periodic  $y$ -direction in order to have well separated growth rates for the modes  $m = 1, 2, 3$ , where  $m$  is the mode number along  $y$  and  $m = 2$  corresponds to the Fast Growing Mode (FGM) of the K-H instability. The values of the sound and Alfvén Mach numbers are set as  $M_s = U_0/C_s = 1.0$ ,  $M_{A,\perp} = U_0/U_{A,\perp} = 1.0$ ,  $M_{A,\parallel} = U_0/U_{A,\parallel} = 20.0$ , with  $U_0 = 1.0$  and  $U_{A,\perp}, U_{A,\parallel}$  the  $z$  and  $y$  component of the equilibrium Alfvén velocity. This choice allows the K-H instability to develop into highly rolled-up vortices. We take  $d_e^2 = 1/64$ . The equations are integrated numerically and numerical stability is achieved by means of filters [18]. Concerning the boundary conditions in the inhomogeneous  $x$ -direction, we note that the K-H vortices are mainly large scale MHD structures. Therefore, even if in the central region the system spontaneously develops smaller scale, higher frequency phenomena which obey a two-fluid dynamics, far from the center towards the boundaries we expect that the plasma dynamics remains of the MHD type. For this reason, at the  $x$ -boundaries we have implemented the projected characteristic decomposition obtained for the hyperbolic MHD set of equations [19, 20]. This allows us to have transparent boundary conditions even for our two-fluid system of equations.

In Fig.1 we show the nearly *frozen-in* magnetic field lines and a plasma passive tracer, advected by the velocity field, used in order to label the plasma domains

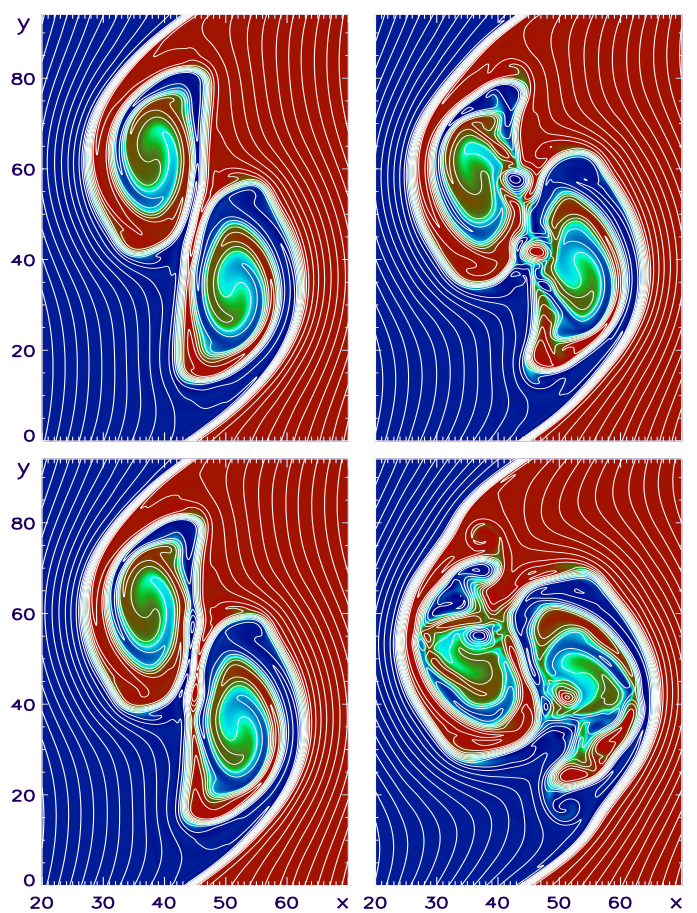


FIG. 1: Plasma passive tracer and magnetic field lines in the  $(x, y)$  plane at  $t = 426, 435$  (left column), and  $t = 450, 480$  (right column).

initially on the right and on the left of the velocity null line. In the first frame (upper-left), we see the two vortices generated by the K-H instability, corresponding to the FGM  $m = 2$ . As soon as the system enters the non-linear phase, the vortices start to pair following an inverse cascade process typical of 2D fluid systems. The good correlation between the plasma and the magnetic structures indicates that the magnetic field is still advected by the fluid velocity. In the first frame we see that the blue and the red domain are well separated by a *ribbon* (white in the figure) of nearly parallel, compressed magnetic lines. This ribbon is rolled-up by the rotation of the two vortices and forms, inside the folds between the vortices, two current layers corresponding to two local magnetic inversion lines. We also see the formation of a first couple of  $X$ -points (one for vortex) in this region at  $x_1 = 44, y_1 = 65$  and at  $x_2 = 45, y_2 = 35$ , respectively. This is the first reconnection event observed in our simulation. At  $t=435$  we show in the second frame (left-bottom) the formation of a second pair of  $X$ -points (one for vortex) in the same inversion region ( $x_3 = 44, y_3 = 50$  and  $x_4 = 45, y_4 = 47$ ). Magnetic reconnection

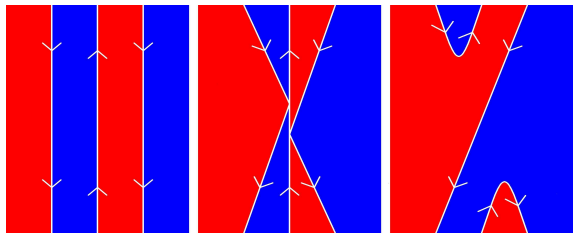


FIG. 2: Schematic representation of the magnetic field lines topology in the region between the two pairing vortices. The lines shown represent the local features of the field line ribbon in Fig.1: the inverted magnetic field lines at  $t = 426$ , the formation of the second pairs of  $X$ -points at  $t = 435$  and the formation of a new magnetic line connection at  $t = 450$ .

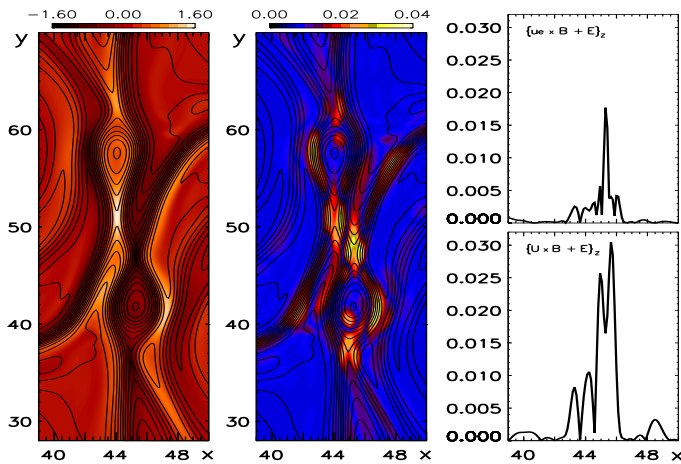


FIG. 3: Left frame: shaded isocontours of the perpendicular current density and magnetic field lines in the region between the two pairing vortices at  $t = 440$ . Central frame: Ion decoupling region ( $D_i \neq 0$ ) and magnetic field lines in the same region at  $t = 440$ . Right frame: Electron (top) and ion (bottom) decoupling region ( $D_e \neq 0$  and  $D_i \neq 0$ , respectively) along the  $x$ -direction at  $y = 47$ ,  $t = 440$ .

develops at these  $X$ -points and forms magnetic islands with typical size  $\sim d_i$ , the maximum value compatible with the dimension of the current sheet. At the same time, the field line ribbon between the second pair of  $X$ -points shrinks and finally opens up. A new ribbon of field lines appears at  $t = 450$ , right top frame. This new ribbon no longer separates the red and the blue plasma regions. Indeed, during this process, significant portions of the red plasma have been engulfed in the form of "blobs" into the blue plasma region and viceversa (right-bottom). The observed change in the large scale magnetic field topology is illustrated in Fig.2, a schematic representation of the region between the two pairing vortices. The inflow plasma velocity at the second pair of  $X$ -points is approximately 0.1 times the value of the local Alfvén velocity  $U_a$  in the  $x$ - $y$  plane, in agreement with the values of the inflow velocity expected in the case of fast magnetic reconnection[1]. Then, the growth rate  $\gamma$  of magnetic re-

connection is inferred to be  $\gamma \sim 0.1 U_a/L \sim 0.15$ , where  $L$  is the shear-length of the in-plane magnetic field at the  $X$ -points. This value is compatible with our estimate of  $\gamma \sim d \ln E_z / dt$  at the  $X$ -point. Note that **the position of the  $X$ -point does not change appreciably and that** in the time interval given by a few growth times of the reconnection instability the two vortices can only rotate by a few degrees so that the current rearrangement caused by the vortex rolling up is not sufficient to interfere with the development of the reconnection process.

In Fig.3, left frame, we show the shaded isocontours of the perpendicular current density  $\mathbf{J}_z$  in the region between the two pairing vortices at  $t = 440$ . We see the two current layers between the vortices at the two magnetic inversion lines where the first and the second pairs of  $X$ -points were formed. The absolute maximum value of the current density in these sheets is in normalized units  $\sim 1.5$  and the width of the sheets is approximately  $0.7d_i$ . Thus we expect the Hall term to be comparable to the  $\mathbf{U} \times \mathbf{B}$  term in Ohm's law. In order to underline its role, we define two quantities,  $D_i = |\{\mathbf{U} \times \mathbf{B} + \mathbf{E}\}_z|$  and  $D_e = |\{\mathbf{u}_e \times \mathbf{B} + \mathbf{E}\}_z|$ , which measure respectively the ion and the electron "decoupling" from the magnetic field. In Fig.3, central frame, we show a wide ion decoupling region where  $D_i \neq 0$ . This region extends across the  $X$ -points over few  $d_i$  lengths. In the right frames of the same figure, we plot a section at  $y = 47$  of  $D_i$  (bottom) and of  $D_e$  (top) at  $t = 440$  and show two separate decoupling regions [1], the "wider" ion decoupling region where  $D_i \neq 0$  and  $D_e \simeq 0$  and the inner, thinner electron decoupling region where  $D_e \neq 0$  of width of the order of a few  $d_e$ . Inside the ion decoupling region, of width roughly equal to  $1.5d_i$ , the magnetic field is essentially frozen in the electron motion but the MHD frozen-in law is not satisfied and the two terms  $\mathbf{U} \times \mathbf{B}$  and  $\mathbf{J} \times \mathbf{B}$  have approximately the same absolute value. Inside the thinner electron region also the electrons are decoupled from the magnetic field and magnetic reconnection can take place.

Finally, we observe that the energy associated to the in-plane magnetic field increases, essentially during the non-linear evolution, by a factor 10.

The crucial role of Hall term has also been demonstrated by running again the same simulation parameters simply omitting the Hall term in the generalized Ohm law. Although the large scale motion of the vortices is still able to generate current sheets of comparable intensity and width, the process of magnetic reconnection is slower. In particular it does not succeed in forming the second pair of  $X$ -points in Fig.1 quickly enough. The two vortices continue to roll-up while pairing and develop into a different magnetic pattern where magnetic islands are eventually generated all over the vortices leading to the disruption of the vortices, as shown in Fig.4. The inferred growth rate at the  $X$ -point located at  $x = 46$ ,  $y = 53$  is  $\gamma \sim 0.08$ . The final topology of the magnetic field is qualitatively different: in the previous case the

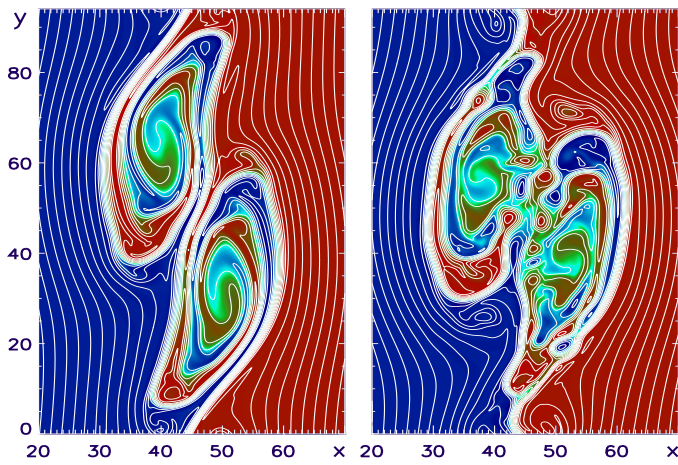


FIG. 4: Shaded isocontours of a plasma passive tracer and magnetic field lines in the  $(x, y)$  plane at  $t = 455,500$  for the parameters of Fig.1, but with the Hall term omitted.

reconnection process occurring at the second pair of  $X$ -points leads to the formation of a global new magnetic connection as illustrated in Fig.2, thus to a single paired vortex. On the contrary, when the Hall term is neglected, no new global magnetic connection is established in the final configuration.

The competition between the development of the large scale magnetic configuration and the evolution and the reconnection instability determines the development of the entire system. If magnetic reconnection is not fast enough, the rolling up of the vortices destroys the favorable conditions for the reconnection instability to grow. **We express the time change of the reconnected flux function, i.e. the difference  $\delta\psi$  between the values of the flux function  $\psi$  of the in-plane magnetic field at the  $X$ -point and at the  $O$ -point, in units of the vortex rotation time  $\tau$  for the island at  $x = 44, y = 57$  in Fig.1 (left-bottom) and for the island at  $x = 46, y = 57$  in Fig.4. We find that in the first case  $\delta\psi$  grows and saturates in approximately  $\tau/8$  while in the second case, where the Hall term is absent, the island forms later and  $\delta\psi$  grows on a slower time scale. In summary, the early evolution of the vortices is essentially MHD and depends only on the initial velocity and magnetic field, regardless of the specific small scale physics included in the generalized Ohm's law. On the contrary, when magnetic reconnection starts to act, the evolution of the whole system depends on the specific physical phenomena that occur at small spatial scales. Large scale physics build up the favorable conditions for reconnection to occur which in turns influences the evolution of the whole system.**

The role of the Hall term has also been demonstrated by running the same simulation parameters with a resis-

tive Ohm's law (without electron inertia) with the Hall term  $\mathbf{E} + \mathbf{U} \times \mathbf{B} - \mathbf{J} \times \mathbf{B} = \eta \mathbf{J}$ , and without the Hall term (resistive MHD)  $\mathbf{E} + \mathbf{U} \times \mathbf{B} = \eta \mathbf{J}$ . Results analogous to those obtained in the case of dissipationless reconnection are obtained for intermediate values of the normalized resistivity  $\eta$  ( $\eta \sim 0.002$ , which is compatible with the estimate  $\eta \simeq \gamma d_e^2$ ). For higher values of the resistivity ( $\eta \sim 0.01$ ) magnetic diffusion effects become too important. Since the magnetic field lines are no longer well frozen in the fluid motion, the large scale motion of the vortices cannot generate current sheets of comparable intensity and width. The vortex motion can no longer lead to the required configuration for fast magnetic reconnection to occur, with or without the Hall term in generalized Ohm's law. On the contrary, if the value of resistivity is smaller ( $\eta \sim 0.001$ ) the vortex motion is able to generate such current sheets, but the process of magnetic reconnection is too slow, again independently of the Hall term. In this case the two vortices continue to roll-up while pairing and develop into a different magnetic pattern where magnetic islands are eventually generated all over the vortices, similar to Fig.4. This behavior is not apparent if we change the magnitude of the electron inertia effects by changing the mass ratio (the values 25, 64, 100 have been considered). This suggests that the fast magnetic reconnection process depends on the small scale mechanism that allows the magnetic field to decouple from the electron fluid.

This work was supported in part by PRIN-MIUR 2006. We are pleased to acknowledge the "Mesocentre SIGAMM" machine, hosted by Observatoire de la Côte d'Azur, where part of the simulations was performed.

- 
- [1] M.A. Shay *et al.*, J. Geophys. Res. **103**, 9165 (1998)
  - [2] D.A. Uzdensky *et al.*, Phys. of Plasmas **13**, 062305 (2006)
  - [3] G. Vekstein *et al.*, Phys. of Plasmas **13**, 122105 (2006)
  - [4] N. Bian *et al.*, Phys. of Plasmas **14**, 072107 (2007)
  - [5] N. Bian *et al.*, Phys. of Plasmas **14**, 120702 (2007)
  - [6] M. Faganello, *et al.*, Phys. Rev. Lett. (2008) in press.
  - [7] A. Otto *et al.*, J. Geophys. Res. **105**, 21175 (2000)
  - [8] H. Baty *et al.*, Phys. of Plasmas **10**, 4661 (2003)
  - [9] T.Nakamura *et al.*, Geophys. Res. Lett. **32**, 21102 (2005)
  - [10] T.Nakamura *et al.*, Adv. Space. Res. **37**, 522 (2006)
  - [11] C. Hashimoto *et al.*, Adv. Space. Res. **37**, 527 (2006)
  - [12] C.D. Winant *et al.*, J. Fluid Mech. **63**, 237 (1974)
  - [13] F.K. Browand *et al.*, J. Fluid Mech.. **76**, 127 (1976)
  - [14] K.W. Min *et al.*, Geophys. Res. Lett. **23**, 3667 (1996)
  - [15] F. Valentini *et al.*, J.Comp. Phys. **225**, 753 (2007)
  - [16] Y. Matsumoto *et al.*, Geophys. Res. Lett. **31**, 2807 (2004)
  - [17] M. Faganello *et al.*, Phys. Rev. Lett. **100**, 015001 (2008)
  - [18] S.K. Lele, J.Comp. Phys. **103**, 16 (1992).
  - [19] K.W. Thompson, J. Comput. Phys., **68**, 1 (1987)
  - [20] S. Landi *et al.*, ApJ, **624**, 392 (2005)